Front. Phys. 13(2), 133701 (2018)
https://doi.org/10.1007/s11467-017-0727-1

RESEARCH ARTICLE

A versatile electrostatic trap with open optical access

Sheng-Qiang Li[1] (李胜强)[†], **Jian-Ping Yin**[2] (印建平)

[1] *School of New Energy and Electronic Engineering, Yancheng Teachers University, Yancheng* 224007, *China*
[2] *State Key Laboratory of Precision Spectroscopy, East China Normal University, Shanghai* 200062, *China*
Corresponding author. E-mail: [†]*lishengqiang_2007@126.com*
Received July 9, 2017; accepted September 13, 2017

A versatile electrostatic trap with open optical access for cold polar molecules in weak-field-seeking state is proposed in this paper. The trap is composed of a pair of disk electrodes and a hexapole. With the help of a finite element software, the spatial distribution of the electrostatic field is calculated. The results indicate that a three-dimensional closed electrostatic trap is formed. Taking ND_3 molecules as an example, the dynamic process of loading and trapping is simulated. The results show that when the velocity of the molecular beam is 10 m/s and the loading time is 0.9964 ms, the maximum loading efficiency reaches 94.25% and the temperature of the trapped molecules reaches about 30.3 mK. A single well can be split into two wells, which is of significant importance to the precision measurement and interference of matter waves. This scheme, in addition, can be further miniaturized to construct one-dimensional, two-dimensional, and three-dimensional spatial electrostatic lattices.

Keywords atomic and molecular physics, electrostatic trap, cold polar molecules, finite element analysis

PACS numbers 37.10.Pq, 37.10.Mn, 37.10.Vz, 37.20.+j

1 Introduction

Cold molecules are of significant importance to scientific research, and have widespread applications in many fields, such as precision measurement [1–3], cold collisions and ultracold chemistry [4–7], quantum computing [8], etc. In recent years, many research groups worldwide have realized the manipulations of cold polar molecules based on the fact that the these molecules feel a force when interacting with an inhomogeneous field. Several theoretical and experimental research works have been developed vigorously, such as electrostatic guiding [9, 10], beamsplitter [11, 12], Stark deceleration [13–15], storage ring [16–18], electrostatic mirror [19], three-dimensional trap [20–22], etc. Moreover, an opened optical access is of considerable importance to an electrostatic well. The molecules trapped in an electrostatic well with an opened optical access can be conveniently detected, cooled, and manipulated [23]. In 2007, a group led by Meijer demonstrated a half-opened AC trap for cold polar molecules [24]. Since 2013, several electrostatic wells with opened optical access have been proposed by the group led by Yin [23, 25]. The shortcoming in both schemes is that only a single well can be formed. However, in researching cold atoms, the splitting and merging of magnetic potential wells has important implications in the interference of matter waves and the in construction of atom interferometers [26–28]. Similarly, the splitting and merging of an electrostatic potential well should find potential applications in atomic and molecular physics.

A versatile electrostatic potential well that has open optical access and can realize splitting and merging of the wells is desired. In the molecular beam experiment, an electrostatic hexapole is usually used for rotational state-selection and orientation of polar molecules [29, 30]. In this paper, we design an electrostatic trap for cold polar molecules in the weak-field-seeking state by using a hexapole and a pair of disk electrodes. Our scheme can realize the conversion between single wells and two asymmetric wells, which have potential applications in the study of superfluids [31, 32].

2 Our scheme

As shown in Fig. 1, our electrostatic potential well is composed of a hexapole and a pair of disk electrodes. To conveniently distinguish the disk electrodes, the teflon

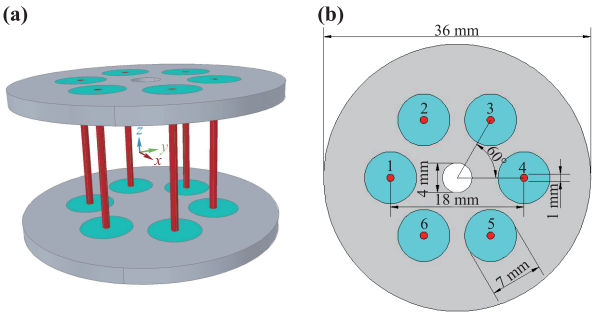

Fig. 1 Schematic diagram of electrostatic trap: **(a)** 3D stereogram and **(b)** top view.

slices, and the hexapole, they are differently colored — gray, cyan, and red, respectively. The teflon slices ($\varepsilon_r = 2.1$) are used as insulation between the hexapole and the disk electrodes. The two disk electrodes are identical, and their thicknesses and diameters are 4 mm and 36 mm, respectively. The distance between the electrodes is 16 mm. The upper electrode is drilled with a hole of 2 mm radius to load the molecular beam into the well. The diameters of the teflon slices are 7 mm, and their centers are drilled with holes of 1 mm diameter. In Fig. 1(b), to avoid confusion and awkward phrasing, each pole of the hexapole was marked from 1 to 6 clockwise. The distance between pole 1 and pole 4 is 18 mm. The voltages applied to the two disk electrodes and six poles of the hexapole are $U_{\rm up}$, $U_{\rm down}$ and U_1, U_2, U_3, U_4, U_5, and U_6.

3 Numerical calculations and Monte Carlo simulations

We choose the ND_3 in the state $|J, K, M\rangle = |1, 1, -1\rangle$ as test molecules, and its Stark potential [23, 33] is

$$W_{\rm Stark} = \sqrt{\left(\frac{W_{\rm inv}}{2}\right)^2 + \left[-\mu E \frac{KM}{J(J+1)}\right]^2} - \frac{W_{\rm inv}}{2}. \quad (1)$$

In the above formula, $W_{\rm inv} = 0.053$ cm^{-1} [34] is the inversion splitting, $\mu = 1.5$ D [35] is the electric dipole moment, E is the magnitude of the electric field, J is the rotational quantum number, and K and M are the projections of the rotational angular momentum on the molecular axis and the external electric field, respectively. As shown in Fig. 2, the distribution of the electric field along the z-axis was calculated using a finite element software (Ansoft Maxwell). A trapping potential is also assigned to the ND_3 molecules in the state, $|J, K, M\rangle = |1, 1, -1\rangle$.

In the loading process, the voltages applied to the electrodes were: $U_{\rm up} = 5$ kV, $U_{\rm down} = 20$ kV, $U_1 = U_3 = U_5 = 25$ kV, $U_2 = U_4 = U_6 = -25$ kV. Then, in the trapping process, the voltages applied to the electrodes

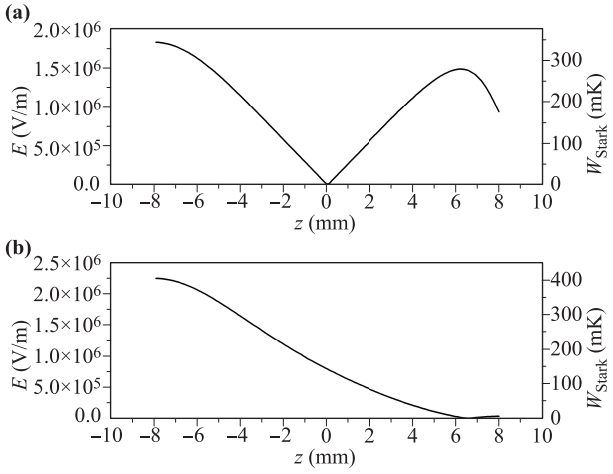

Fig. 2 Distribution of the electrostatic field in the z-direction and the Stark potential of ND_3 molecules during: **(a)** trapping process and **(b)** loading process.

were: $U_{\rm up} = U_{\rm down} = 20$ kV, $U_1 = U_3 = U_5 = 25$ kV, $U_2 = U_4 = U_6 = -25$ kV. As is shown in Fig. 2(a), the electric field along the z-axis is asymmetrical because the lower disk electrode was not drilled. The calculated results indicate that the trapping potential can reach 270 mK for ND_3 molecules. In Fig. 2(b), it can be seen that to load the molecular beam into the electrostatic well, a barrier is needed to decelerate the incident molecules. When the molecules climb up the barrier, their kinetic energy changes to the Stark potential. By the time they get to the center of the well shown in Fig. 2(a), they are decelerated to nearly standstill. Then, the voltage applied is changed from the loading voltage to the trapping voltage. In the simulation, the starting time is the moment the ND_3 molecules begin loading into the trap. Here, $t_{\rm load}$ is a critical point; before $t_{\rm load}$, the molecular beam is gradually decelerated and loaded into the potential well, while after $t_{\rm load}$, the molecules are confined in the electrostatic trap. We simulate the loading and trapping of the molecular beam using the Monte Carlo method. The ND_3 molecules feel a repulsive force in an inhomogeneous electric field, and their motions satisfy Newton's laws of motion:

$$m\ddot{\boldsymbol{r}} = F(\boldsymbol{r}) = -\nabla W_{\rm Stark}(\boldsymbol{r}) \ . \quad (2)$$

Next, the factors affecting the loading efficiency, such as loading time and the initial velocity of incident molecular beam were studied.

As shown in Fig. 3, assuming that the spatial and velocity distributions of the incident molecules are Gaussian, three different incident velocities (8 m/s, 10 m/s, and 12 m/s) were chosen. The full-width at half maximum (FWHM) of the velocity distributions in the x-, y-, and z-directions are all 3 m/s; the central velocities

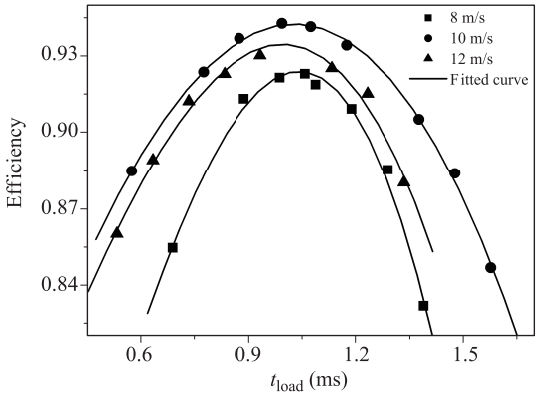

Fig. 3 Relationship between the loading efficiency and the loading time, t_{load}.

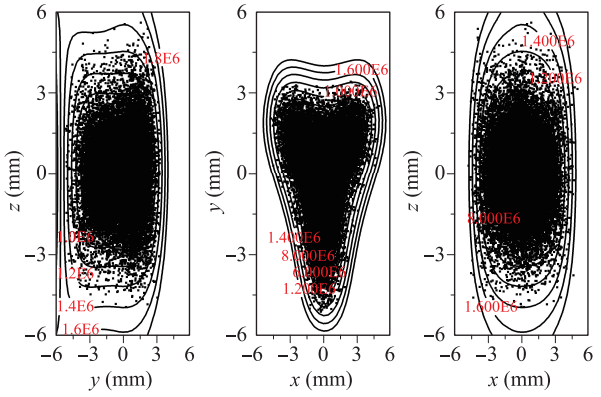

Fig. 5 Contour distribution of the electrical field in three planes, and the positions of the molecules trapped in the well.

in the x-, and y-directions are 0 m/s. It was found that as t_{load} increases, the loading efficiency first increases, then decreases for the three different velocities of the molecular beam. However, there is an optimal loading time at which the maximum loading efficiency can be obtained. When the central velocities of the incident molecular beam are 8 m/s, 10 m/s, and 12 m/s, the optimal loading times are 1.06 ms, 0.9964 ms, and 0.935 ms, respectively; and the maximum loading efficiencies are 92.28%, 94.25%, and 93%, respectively. If the voltages are changed too early, the molecules will not have reached the center of the trap, while if it is too late, the molecules pass through the center of the trap. In both the cases, the molecules cannot be effectively trapped.

From Fig. 3, we infer that the velocities of the incident molecules also significantly influence the loading efficiency. The maximum loading efficiency under several different central velocities of the incident molecular beam (7 m/s, 8 m/s, 9 m/s, 10 m/s, 11 m/s, 12 m/s, and 13 m/s) was obtained. As shown in Fig. 4, when the central velocity of incident molecular beam is 10 m/s, the loading time is 0.9964 ms, and the maximum loading efficiency can reach 94.25%. If the initial velocity is too fast, then as the molecular beam reaches the trap center, the velocity continues to remain high. Even if the molecules are captured, they oscillate intensely, and hence, cannot be trapped well. On the contrary, if the initial velocity is too slow, and the molecules move in the $-z$-direction, then they are decelerated to a standstill before reaching the trap center, and then bounce back in the z-direction. Again, the molecules cannot be trapped effectively.

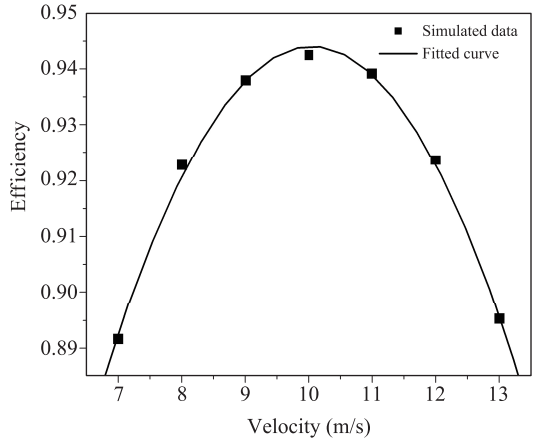

Fig. 4 Relationship between the loading efficiency and the central velocity of the incident molecular beam.

Figure 5 shows the contour distributions of the electric fields in the yOz, xOy, and xOz planes from left to right, in the units of V/m. The points represent the trapped molecules. The number of simulated molecules is 5×10^4. From Fig. 5, we can infer that the molecules are effectively trapped in the three-dimensional, closed, electrostatic potential well.

Thereafter, the temperature of the trapped molecules is calculated. In Fig. 6, the solid square represents the velocity distribution of the initial incident molecular beam, while the solid circle represents the final velocity distribution of the molecules trapped in the well after 0.2 s. It can be seen that the central velocities of the trapped molecules are all 0 in the x-, y-, and z-directions. The FWHMs of the final velocity profile in the x-, y-, and z-directions are 8.36 m/s, 8.34 m/s, and 8.35 m/s, respectively. The corresponding three-dimensional temperature of trapped molecules is about 30.3 mK.

4 Split and merging of the electrostatic trap

The single trap can be transformed into double by varying the voltages applied to the electrodes. The voltages applied to pole 1 and pole 4 are gradually reduced, splitting the single trap into two asymmetrical traps. As shown in Fig. 7, four voltage combinations are chosen

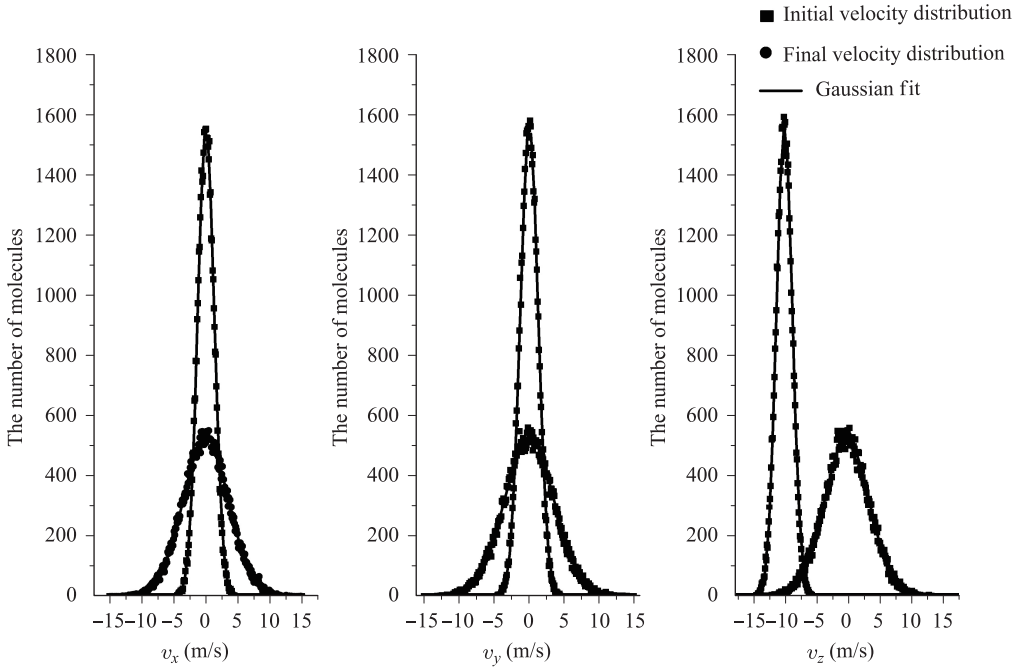

Fig. 6 Velocity distribution of the incident molecular beam and the trapped cold molecules.

— $U_1 = 20$ kV, $U_4 = -20$ kV; $U_1 = 15$ kV, $U_4 = -15$ kV; $U_1 = 15$ kV, $U_4 = 0$ kV; and $U_1 = 15$ kV, $U_4 = 5$ kV. In order to differentiate the four situations, we use solid curve, dash curve, dot curve, and dash-dot curve, respectively. As U_1 and U_4 are changed, the distance between the two wells becomes increases, and the depth of both the wells increases.

The distribution of the trapped molecules in the potential well are then simulated at $U_1 = 15$ kV and $U_4 = 5$ kV.

Figures 8(a) and (b) are the contour distributions of the electric field in the yOz and xOy planes, respectively. The labels in the figures are in units of V/m, and the points are the trapped molecules. It is apparent that the single well has split into two asymmetrical ones.

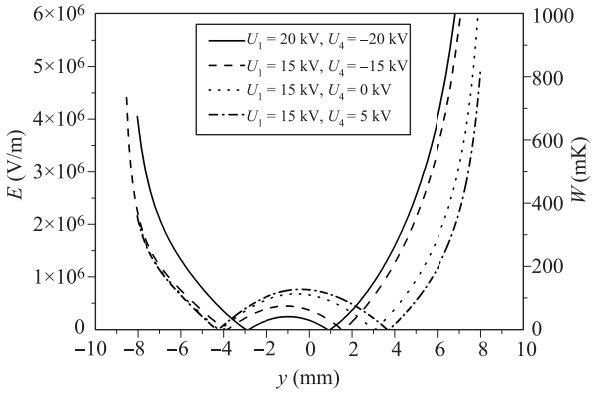

Fig. 7 One-dimensional distribution of the electric field in the y-direction and the trapping potential for ND_3 molecules.

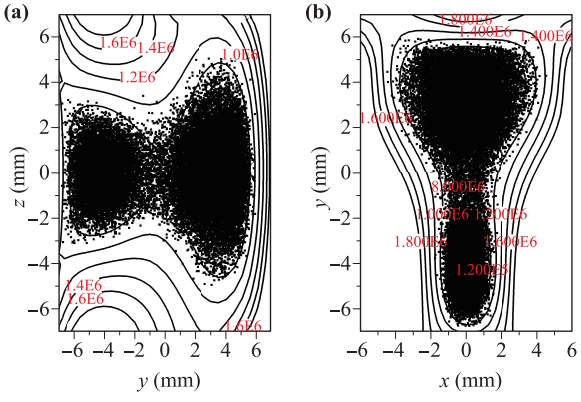

Fig. 8 Contour distributions of the electrostatic field in the **(a)** yOz-plane and **(b)** xOy-plane, including the spatial distribution of the trapped molecules.

5 Electrostatic lattice

Optical lattice has widespread applications such as for polarization gradient cooling and dynamic of trapping [36, 37], Rabi oscillation and Bloch oscillation [38, 39], quantum tunnel effect [40, 41], and Bragg diffraction [42] in an atomic optical lattice. A magnetic lattice also has many applications such as wave packet dynamics;

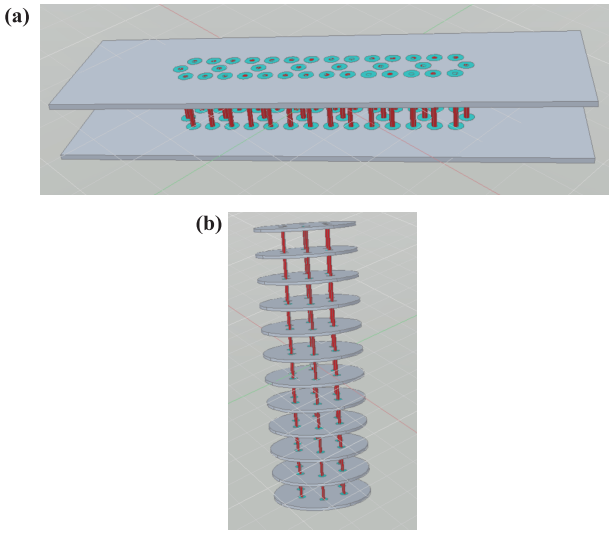

Fig. 9 One-dimensional electrostatic lattices: **(a)** transverse one-dimensional lattice and **(b)** longitudinal one-dimensional lattice.

quantum computing [43]; and one-, two-, and three-dimensional photonic crystals [44–47]. While an optical lattice has an unavoidable photon scattering effect, a magnetic lattice requires cooling of the current coil that produces the magnetic field. An electrical lattice has its own advantages and potential application value.

Our scheme can be further miniaturized to construct one-, two-, and three-dimensional spatial electrostatic lattices.

As shown in Fig. 9(a), our scheme can be further miniaturized (for example, all geometric parameters and the voltages are decreased by an order of magnitude), and repeated in the x- or y-direction to construct a transverse, one-dimensional electrostatic lattice. The cyan and red cylinders represent the teflon slices and the hexapole, respectively. Similarly, our setup in the z-direction can be repeated to form a longitudinal, one-dimensional electrostatic lattice, as is shown in Fig. 9(b).

If our scheme is repeated in two directions (xy, yz, or xz), a two-dimensional electrostatic lattice can be realized. Likewise, if our scheme is repeated in three directions (xyz), a three-dimensional electrostatic lattice can be obtained.

6 Conclusions

In summary, an electrostatic trap with open optical access for cold polar molecules in the weak-field-seeking state using a pair of disk electrodes and a hexapole was designed. By calculating the distribution of the electrostatic field, it can be inferred that a three-dimensional closed electrostatic potential well can be formed. The dynamic processes of loading and trapping the cold molecules were simulated, and the two critical factors affecting the loading efficiency — the loading time and the velocity of incident molecular beam — were studied. The simulated results indicated that when the velocity is 10 m/s and the loading time is 0.9964 ms, the maximum loading efficiency can reach 94.25%, and the corresponding three-dimensional temperature of trapped molecules can reach about 30.3 mK. The conversion of a single well into double was realized by changing the voltages applied to the electrodes; this is of significant importance to precision measurement, matter-wave interference, superfluids, cold chemistry, and cold collisions. Our proposed scheme can be further optimized to construct one-, two-, and three-dimensional spatial electrostatic lattices. Compared to optical and magnetic lattices, electric lattices have their own advantages and potential application value.

Acknowledgements This work was supported by the Young Scientists Fund of the National Natural Science Foundation of China (Grant No. 11504318).

References

1. J. J. Hudson, B. E. Sauer, M. R. Tarbutt, and E. A. Hinds, Measurement of the electron electric dipole moment using YbF molecules, *Phys. Rev. Lett.* 89(2), 023003 (2002)
2. J. Veldhoven, J. Küpper, H. L. Bethlem, B. Sartakov, A. J. A. Roij, and G. Meijer, Decelerated molecular beams for high-resolution spectroscopy, *Eur. Phys. J. D* 31(2), 337 (2004)
3. E. R. Hudson, H. J. Lewandowski, B. C. Sawyer, and J. Ye, Cold molecule spectroscopy for constraining the evolution of the fine structure constant, *Phys. Rev. Lett.* 96(14), 143004 (2006)
4. J. J. Gilijamse, S. Hoekstra, S. Y. T. van de Meerakker, G. C. Groenenboom, and G. Meijer, Near-threshold inelastic collisions using molecular beams with a tunable velocity, *Science* 313(5793), 1617 (2006)
5. S. Willitsch, M. T. Bell, A. D. Gingell, S. R. Procter, and T. P. Softley, Cold reactive collisions between laser-cooled ions and velocity-selected neutral molecules, *Phys. Rev. Lett.* 100(4), 043203 (2008)
6. B. C. Sawyer, B. K. Stuhl, M. Yeo, T. V. Tscherbul, M. T. Hummon, Y. Xia, J. Klos, D. Patterson, J. M. Doyle, and J. Ye, Cold heteromolecular dipolar collisions, *Phys. Chem. Chem. Phys.* 13(42), 19059 (2011)
7. L. P. Parazzoli, N. Fitch, D. S. Lobser, and H. J. Lewandowski, High-energy-resolution molecular beams for cold collision studies, *New J. Phys.* 11(5), 055031 (2009)

8. D. DeMille, Quantum computation with trapped polar molecules, *Phys. Rev. Lett.* 88(6), 067901 (2002)
9. T. Junglen, T. Rieger, S. A. Rangwala, P. W. H. Pinkse, and G. Rempe, Two-dimensional trapping of dipolar molecules in time-varying electric fields, *Phys. Rev. Lett.* 92(22), 223001 (2004)
10. Y. Xia, Y. L. Yin, H. B. Chen, L. Z. Deng, and J. P. Yin, Electrostatic surface guiding for cold polar molecules: Experimental demonstration, *Phys. Rev. Lett.* 100(4), 043003 (2008)
11. L. Z. Deng, Y. Liang, Z. X. Gu, S. Y. Hou, S. Q. Li, Y. Xia, and J. P. Yin, Experimental demonstration of a controllable electrostatic molecular beam splitter, *Phys. Rev. Lett.* 106(14), 140401 (2011)
12. S. D. S. Gordon and A. Osterwalder, 3D-printed beam splitter for polar neutral molecules, *Phys. Rev. Appl.* 7(4), 044022 (2017)
13. H. L. Bethlem, G. Berden, and G. Meijer, Decelerating neutral dipolar molecules, *Phys. Rev. Lett.* 83(8), 1558 (1999)
14. M. Quintero-Pérez, P. Jansen, T. E. Wall, J. E. van den Berg, S. Hoekstra, and H. L. Bethlem, Static trapping of polar molecules in a traveling wave decelerator, *Phys. Rev. Lett.* 110(13), 133003 (2013)
15. S. Y. Hou, S. Q. Li, L. Z. Deng, and J. P. Yin, Dependences of slowing results on both decelerator parameters and the new operating mode: Taking ND_3 molecules as an example, *J. Phys. At. Mol. Opt. Phys.* 46(4), 045301 (2013)
16. F. M. H. Crompvoets, H. L. Bethlem, R. T. Jongma, and G. Meijer, A prototype storage ring for neutral molecules, *Nature* 411(6834), 174 (2001)
17. P. C. Zieger, S. Y. T. van de Meerakker, C. E. Heiner, H. L. Bethlem, A. J. A. van Roij, and G. Meijer, Multiple packets of neutral molecules revolving for over a mile, *Phys. Rev. Lett.* 105(17), 173001 (2010)
18. S. Q. Li, L. Xu, L. Z. Deng, and J. P. Yin, Controllable electrostatic surface storage ring with opened optical access for cold polar molecules on a chip, *J. Opt. Soc. Am. B* 31(1), 110 (2014)
19. S. J. Wark and G. I. Opat, An electrostatic mirror for neutral polar molecules, *J. Phys. At. Mol. Opt. Phys.* 25(20), 4229 (1992)
20. H. L. Bethlem, G. Berden, F. M. H. Crompvoets, R. T. Jongma, A. J. A. van Roij, and G. Meijer, Electrostatic trapping of ammonia molecules, Nature 406(6795), 491 (2000)
21. T. Rieger, T. Junglen, S. A. Rangwala, P. W. H. Pinkse, and G. Rempe, Continuous loading of an electrostatic trap for polar molecules, *Phys. Rev. Lett.* 95(17), 173002 (2005)
22. S. A. Meek, H. Conrad, and G. Meijer, Trapping molecules on a chip, *Science* 324(5935), 1699 (2009)
23. Z. X. Wang, Z. X. Gu, Y. Xia, X. Ji, and J. P. Yin, Optically accessible electrostatic trap for cold polar molecules, *J. Opt. Soc. Am. B* 30(9), 2348 (2013)
24. M. Schnell, P. Lutzow, J. van Veldhoven, H. L. Bethlem, J. Kupper, B. Friedrich, M. Schleier-Smith, H. Haak, and G. Meijer, A linear AC trap for polar molecules in their ground state, *J. Phys. Chem. A* 111(31), 7411 (2007)
25. Z. X. Wang, Z. X. Gu, L. Z. Deng, and J. P. Yin, Cooling and trapping polar molecules in an electrostatic trap, *Chin. Phys. B* 24(5), 053701 (2015)
26. W. J. Mullin and F. Laloe, Interference effects in potential wells, *Phys. Rev. A* 91(5), 053629 (2015)
27. W. Hänsel, J. Reichel, P. Hommelhoff, and T. W. Hansch, Trapped-atom interferometer in a magnetic microtrap, *Phys. Rev. A* 64(6), 063607 (2001)
28. S. J. Kim, H. Yu, S. T. Gang, D. Z. Anderson, and J. B. Kim, Controllable asymmetric double well and ring potential on an atom chip, *Phys. Rev. A* 93(3), 033612 (2016)
29. P. R. Brooks, Reactions of oriented molecules, *Science* 193(4247), 11 (1976)
30. M. Brouard, D. H. Parker, and S. Y. T. van de Meerakker, Taming molecular collisions using electric and magnetic fields, *Chem. Soc. Rev.* 43(21), 7279 (2014)
31. L. J. LeBlanc, A. B. Bardon, J. McKeever, M. H. T. Extavour, D. Jervis, J. H. Thywissen, F. Piazza, and A. Smerzi, Dynamics of a tunable superfluid junction, *Phys. Rev. Lett.* 106(2), 025302 (2011)
32. S. Levy, E. Lahoud, I. Shomroni, and J. Steinhauer, The a.c. and d.c. Josephson effects in a Bose–Einstein condensate, *Nature* 449(7162), 579 (2007)
33. S. Y. T. van de Meerakker, H. L. Bethlem, N. Vanhaecke, and G. Meijer, Manipulation and control of molecular beams, *Chem. Rev.* 112(9), 4828 (2012)
34. L. Fusina and G. D. Lonardo, Inversion-rotation spectrum and spectroscopic parameters of $^{14}ND_3$ in the ground state, *J. Mol. Spectrosc.* 112(1), 211 (1985)
35. G. D. Lonardo and A. Trombetti, Dipole moment of the $v_2 = 1$ state of ND_3 by saturation laser stark spectroscopy, *Chem. Phys. Lett.* 84(2), 327 (1981)
36. G. Raithel, G. Birkl, A. Kastberg, W. D. Phillips, and S. L. Rolston, Cooling and localization dynamics in optical lattices, *Phys. Rev. Lett.* 78(4), 630 (1997)
37. A. Hemmerich, M. Weidemuller, T. Esslinger, C. Zimmermann, and T. Hansch, Trapping atoms in a dark optical lattice, *Phys. Rev. Lett.* 75(1), 37 (1995)
38. M. C. Fischer, K. W. Madison, Q. Niu, and M. G. Raizen, Observation of Rabi oscillations between Bloch bands in an optical potential, *Phys. Rev. A* 58, R2648(R) (1998)
39. M. B. Dahan, E. Peik, J. Reichel, Y. Castin, and C. Salomon, Bloch oscillations of atoms in an optical potential, *Phys. Rev. Lett.* 76, 4508 (1996)

40. C. Jurczak, B. Desruelle, K. Sengstock, J. -Y. Courtois, C. I. Westbrook, and A. Aspect, Atomic transport in an optical lattice: An investigation through polarization-selective intensity correlations, *Phys. Rev. Lett.* 77, 1727 (1996)

41. S. K. Dutta, B. K. Teo, and G. Raithel, Tunneling dynamics and gauge potentials in optical lattices, *Phys. Rev. Lett.* 83(10), 1934 (1999)

42. M. Weidemuller, A. Hemmerich, A. Gorlitz, T. Esslinger, and T. W. Hansch, Bragg diffraction in an atomic lattice bound by light, *Phys. Rev. Lett.* 75(25), 4583 (1995)

43. J. K. Pachos and P. L. Knight, Quantum computation with a one-dimensional optical lattice, *Phys. Rev. Lett.* 91(10), 107902 (2003)

44. J. P. Yin, W. J. Gao, N. C. Liu, J. J. Hu, and Y. Z. Wang, Magnetic guide and trap for cold neutral atoms with current-carrying wires and conductors, *J. Chin. Chem. Soc. (Taipei)* 48(3), 555 (2001)

45. J. P. Yin, W. J. Gao, J. J. Hu, and Y. Q. Wang, Magnetic surface microtraps for realizing an array of alkali atomic Bose–Einstein condensates or Bose clusters, *Opt. Commun.* 206(1–3), 99 (2007)

46. J. P. Yin, W. J. Gao, J. J. Hu, and N. C. Liu, Atomic magnetic lattices and their applications, *Chin. Phys. Lett.* 19(3), 327 (2002)

47. J. P. Yin, W. J. Gao, and J. J. Hu, Arrays of microscopic magnetic traps for cold atoms and their applications in atom optics, *Chin. Phys.* 11(5), 472 (2002)